For the JINR Scientific Works Competition for 2021

PRESENTATION

The following work is presented

"Experimental study of femtoscopic correlations of charged kaon pairs produced in pp, p-Pb and Pb-Pb collisions with the ALICE detector at LHC energies"

Section: Experimental research works.

Team of researchers:

1. Batyunya B.V.
2. Malinina L.V.
3. Mikhaylov K.R.
4. Rogochaya E.P.
5. Romanenko G.E.

The presented series of works is based on experimental results that were obtained in the period from 2010 to 2020 and published as the following eight peer-reviewed papers:

1. B. Abelev et al. (ALICE Collaboration), "Charged kaon femtoscopic correlations in pp collisions at $\sqrt{s}$ = 7 TeV", Phys. Rev. D **87**, 052016 (2013).

2. J. Adam et al. (ALICE Collaboration), "One-dimensional pion, kaon, and proton femtoscopy in Pb–Pb collisions at $\sqrt{s_{\mathrm{NN}}}$ = 2.76 TeV", Phys. Rev. C **92**, 054908 (2015).

3. L. Malinna (for ALICE Collaboration), "Femtoscopy of identified particles in Pb-Pb collisions with ALICE at the LHC", Nucl. Phys. A **00** (2015) 1-4.

4. K. Mikhaylov, "Bose-Einstein correlations of charged and neutral kaons in pp and Pb-Pb collisions at the LHC with the ALICE experiment", Journal of Physics: Conference Series **668** (2016) 012071.

5. S. Acharya et al. (ALICE Collaboration), "Kaon femtoscopy in Pb-Pb collisions at $\sqrt{s_{\mathrm{NN}}}$ = 2.76 TeV", Phys. Rev. C **96,** 064613 (2017)

6. S. Acharya et al. (ALICE Collaboration), **"**One-dimensional charged kaon femtoscopy in p-Pb collisions at $\sqrt{s_{\mathrm{NN}}}$ = 5.02 TeV", Phys. Rev. C **100**, 024002 (2019)

7. K. Mikhaylov, "Non-identical charged kaon femtoscopy in Pb-Pb collisions at $\sqrt{s_{\mathrm{NN}}}$ = 2.76 TeV by ALICE", Journal of Physics: Conference Series. **1690**, 012099 (2020).

8. B. Batyunya, L. Malinina, K. Mikhaylov, E. Rogochaya, G. Romanenko, K. Werner, "Identical pion and kaon femtoscopy in EPOS 3 with and without the hadronic afterburner UrQMD"**,**

Journal of Physics: Conference Series. **1690**, 012102 (2020).

In the listed ALICE Collaboration publications, the Paper Committee consisted either fully of physicists from JINR or also included physicists from other institutes, like in [2, 5] where the analyses were performed in collaboration.

The presented results were reported at more than 20 international conferences. Here the list of the most known and prestigious of them is shown:

- L. Malinina, "Charged KK femtoscopy correlations from 7 TeV pp collisions", poster. International Conference of Quark Matter 2011 (Annecy, France), 23.05-28.05.

- E. Rogochaya, "Kaon femtoscopy correlations in Pb-Pb collisions at $\sqrt{s_{\mathrm{NN}}}$ = 2.76 TeV from the ALICE experiment at LHC", XXI International Baldin Seminar on High Energy Physics Problem, September 10-15, 2012.

- K. Mikhaylov, "Charged kaon femtoscopy in interactions at $\sqrt{s}$ = 7 TeV ", XIII GDRE Workshop on Relativistic Heavy Ion Physics, Nantes 2012.

- L. Malinina, “Kaon femtoscopy of Pb-Pb and pp collisions at the LHC with the ALICE.”, International Conference on New Frontiers in Physics, Crete, 2013.

- L. Malinina, “Correlation femtoscopy with ALICE”, International Conference-Section of Nuclear Physics of the Physical Sciences Division of the Russian Academy of Sciences, Moscow, November 2014.

- L. Malinina, “Femtoscopy of identified particles in Pb-Pb collisions with ALICE at the LHC”, XXV International Conference of Quark Matter (QM-2015), Kobe, Japan.

- K. Mikhailov (JINR), “Bose-Einstein correlations of charged and neutral kaons in pp and Pb-Pb collisions at LHC with ALICE experiment“, The 15h International Conference on Strangeness in Quark Matter (SQM-2015), Dubna.

- K. Mikhaylov, “Identical and non-identical kaon correlations in pp and Pb-Pb at LHC.”, GDRE Workshop, Subatech, Nantes, July 2016.

- E. Rogochaya (JINR), “Charged kaon femtoscopy correlations in p-Pb collisions at 5.02 TeV with ALICE at the LHC”, XII WPCF, June 2017, Amsterdam.

- K. Mikhaylov, “Non-identical kaon femtoscopy with ALICE experiment”, XX GDRE Workshop, Subatech, Nantes, July 2018.

- K. Mikhaylov, “$K^{+}K^{-}$ correlations in Pb-Pb collisions at $\sqrt{s_{\mathrm{NN}}}$ = 2.76 TeV by ALICE at the LHC” XIV WPCF, Dubna, Russia, 2019.

- L. Malinina (JINR, SINP MSU, on behalf of the ALICE Collaboration), “Femtoscopic correlations of identical charged particles in pp collisions at LHC energies with event-shape selection**”,** 5th International Conference on Particle physics and Astrophysics (ICPPA-2020), October 7, 2020, MEPhI, Moscow.

In addition, the results of the group were included in various reports given at JINR seminars:

- B.V. Batyunya, «ALICE (A Large Ion Collider Experiment) results at the LHC", Seminar VBLHEP, 31.10.2012; Seminar BLTP, 19.02.2014; Seminar JINR, 07.06.2017; Seminar VBLHEP, 08.02.2019.
- L.V. Malinina, "Femtoscopy of heavy-ion and pp collisions at high energies", Seminar BLTP, 2014.

Introduction.

The ALICE is a multipurpose experiment to investigate the interactions of heavy ions, which was created to study the physics of strongly interacting matter, the quark-gluon plasma (QGP) in nucleus-nucleus collisions at the CERN LHC. In addition to the main topic, an extensive program is being carried out to study proton-proton and proton-nuclear collisions, primarily for comparison with the results of heavy-ion collisions.

It was assumed in the beginning of 80s of the last century that the extremely high-energy densities achieved in the collisions of heavy nuclei (A-A) may entail the formation of the QGP, state of matter characterized by partonic degrees of freedom (quark deconfinement) [9]. Twenty years later, in 2000, the convincing arguments of such a matter state existence were presented in the special CERN seminar according to the data obtained in some experiments at the SPS accelerator. It was also assumed [10] that a local QGP production in the mixed quark-hadron phase has been observed at the reached energy. The full QGP stage may be achieved at larger collision energy density with increasing collision energies that would lead to stronger signatures of the QGP.

In hydrodynamic models, the highly compressed strongly-interacting system in A-A collisions is expected to undergo longitudinal and transverse expansions, defined a size of the particle emitting source. Experimentally, such expansion can manifest itself through Bose-Einstein correlations for pairs of identical particles [11, 12] or through correlations of pairs of non-identical particles due to interactions in the final state [13]. These correlations are known now as femtoscopic correlations. The JINR group widely participates in these investigations, mostly of charged kaon pairs produced in pp, p-Pb and Pb-Pb collisions. Such a choice was primarily due to the traditional interest of JINR physicists in this area, which began with the "pioneer" works in the 70s of the last century by JINR theorists G. I. Kopylov and M. I. Podhoretsky [12]. JINR physicists V.L. Luboshits and R. Lednitsky [13] took an extensive part in the further theoretical development, the latter of whom is currently one of the widely recognized specialists in the world in this field. The second reason for choosing the kaon analysis is due to the relatively small number of such results compared to the numerous data on the study of pion pairs at different energies. For example, the results of studying pairs of charged kaons in pp and p-A collisions at lower energies were generally absent, most likely due to insufficient statistics of well enough identified kaons. Finally, another advantage of the study of kaon pairs in comparison with pion pairs is a weaker influence of the decays of resonances, which in this case are considered as background processes.

1. Study of charged kaon femtoscopic correlations in pp collisions at $\sqrt{s}$ = 7 TeV [1].

In this study, approximately 300 mln. events obtained in pp collisions at the LHC in 2010 were analyzed. The description of the detectors, the method of event selection, selection and reconstruction of particle tracks and particle identification is given in sufficient detail in [1]. Here we briefly note that the selection of events was performed using the minimum-bias trigger with only checking whether the selected events belonged to a pp collision. The tracks were reconstructed using the Inner Tracking

System of silicon detectors and a Time-Projection Chamber (TPC), and then the track parameters were determined by the Kalman filter method. The necessary efficiency of kaon identification was obtained by measuring energy losses in the TPC and the time of flight in the Time-of-Flight detector (TOF) for particles of different types. The purity of selected kaons (the ratio of correctly identified kaons to all particles reconstructed as kaons) was determined by the Monte Carlo simulation method using a detailed simulation of detectors and generators of interactions under consideration. The analysis of experimental and simulated data was carried out within the framework of the ALIROOT software package developed in ALICE. Figure 1 shows the dependence of the selected kaon purity and the fraction of contamination from pions and electrons on the transverse momentum of kaons in the TPC (at $p_T < 0.6$ GeV/c) and in the TOF (at $p_T > 0.6$ GeV/c). It can be seen that the biggest contamination comes from electrons in the p_T range of (0.35-0.60) GeV/c. The contamination related to kaon pairs was estimated of the same order. It should be noted that this contamination only reduces the correlation strength and does not affect the shape of the correlation function. The correlation function was determined using the ratio CF ($\mathbf{p}_1$,$\mathbf{p}_2$) = A($\mathbf{p}_1$,$\mathbf{p}_2$)/B($\mathbf{p}_1$,$\mathbf{p}_2$), where A($\mathbf{p}_1$,$\mathbf{p}_2$) is the two-particle distribution in the analyzed event and B($\mathbf{p}_1$,$\mathbf{p}_2$) is the reference distribution constructed by mixing particles from different events, and $\mathbf{p}_1$, $\mathbf{p}_2$ are the three-momenta of particles 1 and 2, respectively. Commonly the correlation function is considered depending on the invariant pair relative momentum $q_{inv} = (|\mathbf{q}|^2 - q_0^2)^{1/2}$, $\mathbf{q} = \mathbf{p}_1 - \mathbf{p}_2$, $q_0 = E_1 - E_2$.

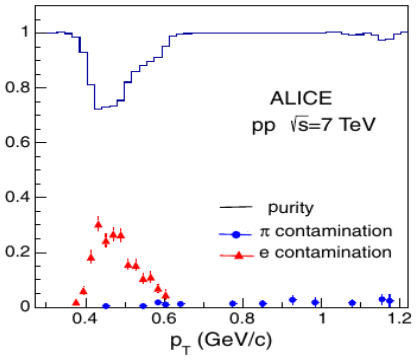

Fig. 1: Purity and contamination of selected charged kaons in the Monte Carlo simulation.

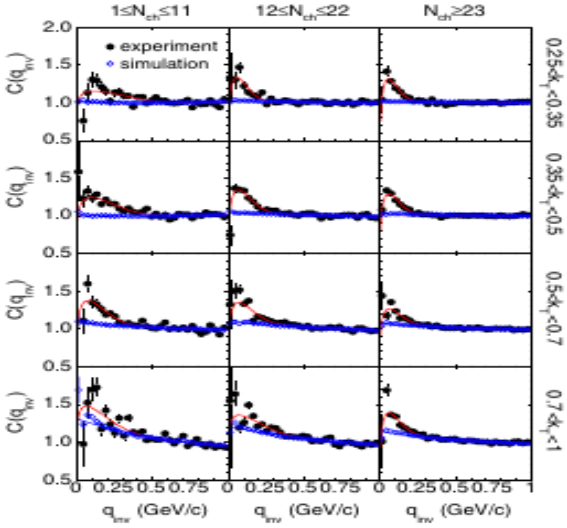

Fig. 2: Correlation functions of charged kaon pairs in pp collisions.

It is shown by black solid circles in Fig. 2 in several charged particle multiplicity N_{ch} bins and different intervals of the half of the pair transverse momentum $k_T = |\mathbf{p}_{T,1} + \mathbf{p}_{T,2}|/2$. Blue empty circles show the correlations obtained using the PYTHIA-PERUGIA-2011 Monte Carlo generator. The presented correlation functions are normalized to unity at $q_{inv} > 0.5$ GeV/c outside the region of the correlation effect peak. The results are obtained summing up pairs of positively and negatively charged kaons, the correlation functions for which coincide within uncertainties. It can be seen that at $q_{inv} > 0.5$ GeV/c, the experimental data are well described by the model where there are no femtoscopic effects included and where an increase in the correlation function with increasing k_T at small q_{inv} is presumably due to the influence of mini-jets. The correlation function was fit with the one-dimensional Gaussian function [14]:

$$CF(q_{inv}) = \{1 - \lambda + \lambda K(q_{inv})[1 + \exp(-R_{inv}^2 q_{inv}^2)]\} \cdot D(q_{inv}), \quad (1)$$

where the parameters λ and R_{inv} are the correlation strength and the radius of the source emitting kaons, $K(q_{inv})$ is the Coulomb function. The function $D(q_{inv})$ describes the so-called baseline, which takes into account all non-femtoscopic correlations including the mini-jets mentioned above and long-lived correlations due to the energy-momentum conservation law. The results of the fit by Eq. (1) are shown by the red line in Fig. 2. The baseline used in the fit was obtained from the Monte Carlo data fit with a second-order polynomial (blue line).

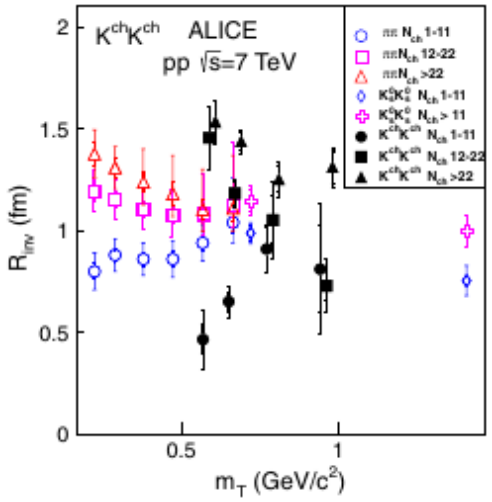

Fig. 3: Radii of particle radiation sources depending on the m_T for different multiplicities of events.

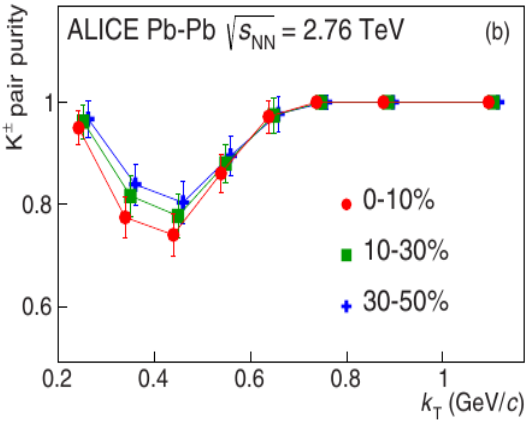

Fig. 4: Purity of identification of charged kaon pairs depending on k_T in Pb-Pb collisions of different centralities.

Figure 3 shows the dependences of R_{inv} on the pair transverse mass $m_T = (k_T^2 + m_K^2)^{1/2}$ where m_K is the mass of the kaon. As noted above, such data for charged kaons were obtained in pp collisions for the first time, so the comparison was made with the results obtained in ALICE at the same energies for pairs of charged pions [15] and neutral kaons ($K^0_sK^0_s$) [16] also shown in Fig. 3. As seen from the comparison, R_{inv} increase with increasing N_{ch} for all types of pairs. The radii R_{inv} decrease at N_{ch} >11 with increasing m_T. However, at less charged particle multiplicities, the radii for charged mesons show the opposite trend and increase with increasing m_T. This effect is quantitatively stronger for kaon pairs than for pion ones. It is interesting to note here that the decrease of R_{inv} in A-A collisions is explained by the influence of a strong collective hydrodynamic expansion in the created matter [17]. Such decrease of R_{inv} in pp collisions is also associated with the possible influence of the hydrodynamic phase, the contribution of which is very small at small N_{ch} values [18]. It should be noted that the possible manifestation of collective effects in the formation of small systems in pp and p-Pb collisions with increasing multiplicity of charged particles is also discussed on the basis of such observations as the "ridge" effect (CMS, LHC) [19] and an increase in the production of strange particles with increasing multiplicity of events (ALICE) [20]. Figure 3 also shows that R_{inv} is larger for kaons than for pions at the same m_T and N_{ch} > 11. According to the model [21], such an excess may be due to less influence of resonance decays for kaons than for pions.

As was said above, the parameter λ in Eq. (1) characterizes the correlation strength. It equals unity in an ideal case of pure femtoscopic correlations and is always less than unity in any real experiment. Possible reasons include partial coherence of particle emission sources [22], the contribution of particles from decays of long-lived resonances, deviation of the correlation function shape from the Gaussian parametrization, imperfect identification of particles. In the presented analysis, the value of λ varied in the (0.3-0.5) range.

2. Study of femtoscopic correlations of charged kaons in Pb-Pb collisions.

In the late 80s and in the 90s of the last century, predictions were made within the framework of hydrodynamic models [23, 24] about significant space-time extension of the resulting fireball (a source of particle emission) in A-A collisions due to the influence of QGP at energies of RHIC and LHC accelerators. However, this prediction was not confirmed experimentally, which was called "HBT puzzle" [25]. The solution of the problem was found with the further development of models [26-28] taking into account such factors as transverse particle flows at the initial stage of interactions, the transition from the QGP to the hadron phase through the "crossover" mechanism, the phase of the hadron cascade. The production of kaons was also interesting because of the possibility to compare the radii of their emission sources with the sources of other particles, including checking the predicted [29, 30] universal dependence of the radii for various particle types on m_T (so-called m_T scaling).

2.1. One-dimensional analysis of femtoscopic correlations of charged kaon pairs in Pb-Pb collisions at $\sqrt{s_{NN}}$ = 2.76 TeV [2, 4].

The analysis indicated in the title was carried out in collaboration with other groups to compare the femtoscopic parameters of charged kaons with the parameters of other particle species. The method of selecting events and particles was similar to the one described in Section 1. The only difference was the identification of kaons in the TPC, which consisted in fitting the experimental distributions of energy losses of particles in different momentum intervals with a triple Gaussian function to separate kaon signals from the signals of electrons and pions. The purity of identification of kaon pairs as a function of k_T is shown in Fig. 4 and was determined using the purities of single kaons shown in figure 1 in [4]. This method made it possible to determine more precisely the purity of the kaon selection and the contamination, which, as in the case of pp collisions, was determined mainly by the contribution of electrons. The correlation functions were corrected taking into account the momentum resolution of the particles by the method described in [2]. Figure 5 shows an example of a correlation function with uncertainties which are mostly systematic. The curve is the result of fitting with the Formula (1), in which the function $D(q_{inv})$ was equal to unity. Figure 6 shows the radii of sources for pairs of different particle species depending on $<m_T>$ for collisions of different centralities. It can be seen that the radii increase for more central events, which is expected from a simple geometric picture of particle collisions. The effect of decreasing radii with increasing $<m_T>$ is observed and was discussed in Section 1. The m_T scaling mentioned above is also seen for kaon and proton/antiproton pairs within uncertainties.

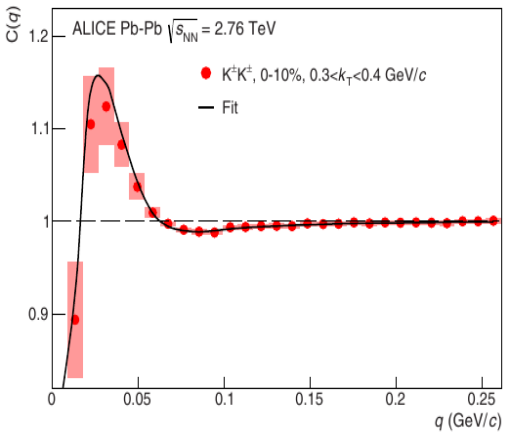

Fig. 5: Correlation function of identical charged kaon pairs. The line is the result of fitting with the Formula

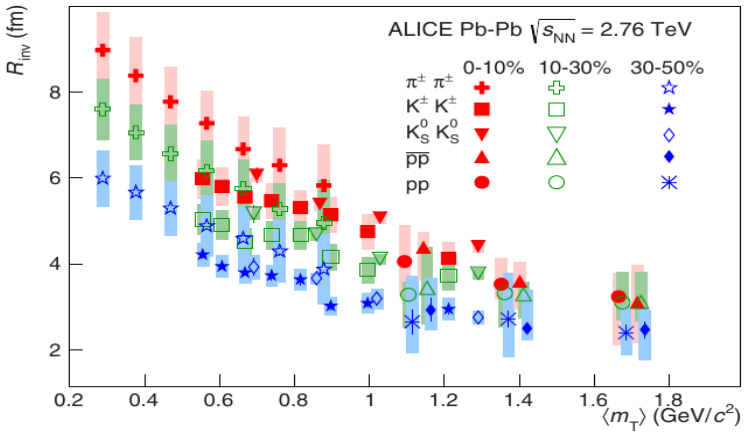

Fig. 6: Radii of particle emission sources depending on $<m_T>$ for collisions of different centralities.

(1).

The violation of m_T scaling for pion pairs can be explained [30] by an increasing influence of the Lorentz factor with the decreasing mass of particles during the transition from the Longitudinally Co-Moving System (LCMS) for which the prediction was made to the Pair Rest Frame (PRF) in which the analysis is performed.

2.2. Three-dimensional analysis of femtoscopic correlations of identical charged kaon pairs in Pb-Pb collisions at $\sqrt{s_{NN}}$ = 2.76 ТэВ [3, 5].

Three-dimensional analysis of femtoscopic correlations allows one to study in more detail the three components of the radius of the particle emitting source, i.e., in fact, the spatial shape of the source. In this analysis, the main attention was paid to checking the mechanisms of particle production considered in various models considering m_T scaling, which was discussed in Section 2.1. The experimental technique in this analysis was the same as in the one-dimensional analysis discussed above. The correlation function in three-dimensional analysis is represented as depending on three components of the variable q (specified in Section 1), which are calculated in the LCMS system where the longitudinal momentum of the pair is equal to zero and the projections q_{out}, q_{side}, q_{long} are determined as follows: "long" – along the beam, "out" – along the transverse momentum of the pair, "side" – perpendicular to the latter in the transverse plane. In this case, the three-dimensional correlation function was fit with the formula [14]:

$$C(\mathbf{q}) = N(1-\lambda) + N\lambda K(q)\left[1 + \exp\left(-R_{out}^2 q_{out}^2 - R_{side}^2 q_{side}^2 - R_{long}^2 q_{long}^2\right)\right], \quad (2)$$

where R_{out}, R_{side}, R_{long} are Gaussian femtoscopic radii in LCMS, N is a normalization parameter, and q is calculated in PRF. The parameter λ and the Coulomb function $K(q)$, like in Eq. (1), describe the correlation strength and the Coulomb interaction of charged particles, respectively.

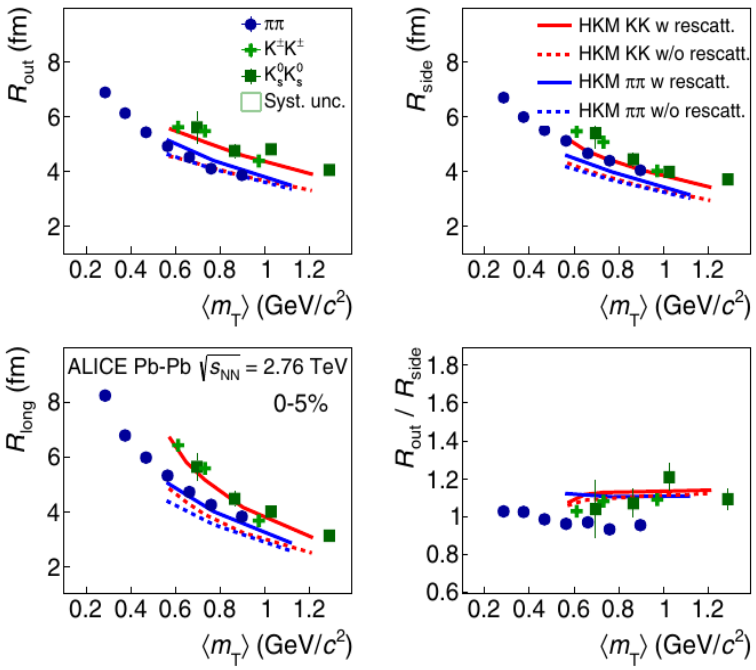

Fig. 7: The dependence of the three components of the radii and the ratio of the radii in the transverse plane of the emission sources of pions and kaons on the average transverse mass of particle pairs <m_T>. The curves are the result of the prediction of the HKM model taking into account (w rescatt) and without taking into account (w/o rescatt) the rescattering of particles at the hadron phase stage.

The projections of the correlation functions on the "out", "side", "long" axes, depending on q_{out}, q_{side},

q_{long}, respectively, are shown in figure 2 in [5] where the results of fitting with the Formula (2) are also given. Figure 7 here compares the values of R_{out}, R_{side}, R_{long} obtained by such fitting and the R_{out}/R_{side} ratio depending on $\langle m_T \rangle$ for pions and kaons (charged and neutral) formed in the most central Pb-Pb collisions (0-5%). It can be seen that the radii for kaons are noticeably larger than for pions at the same values of m_T, i.e. m_T scaling is not observed. The lines in the figure show the results of the prediction of the hydrokinetic model (HKM) [31] with (w rescatt) or without (w/o rescatt) the rescattering of particles in the final state. From the physical point of view, the second case (an early version of the model) predicts an instantaneous transition from the QGP to the final state when free particles are registered in the detectors. At the same time, the model does not describe (dotted lines) violations of m_T scaling. The same result is obtained in another similar model (THERMINATOR-2) [30] as can be seen from figure 4 in [5]. Taking into account the rescattering of hadrons before the freeze-out of particles leads to agreement with the experimental data (solid lines in Fig. 7). The same results were obtained (shown in figure 2 in [8]) when compared with another hydrodynamic model EPOS-3, which differs from HKM in some details of the initial conditions of particle interaction described in the framework of the Monte Carlo-Glauber approach in HKM and the Gribov-Regge parton scattering approach in EPOS-3. This comparison of the experimental data with the models demonstrates the importance of taking into account the rescattering of particles in the final state during hadronization. As seen from Fig. 7, the ratios R_{out}/R_{side} are close to unity both for pions and kaons. A good description of this ratio, as well as the source radii, by the models was also possible when considering the initial stage of interaction of nuclei before the thermal equilibrium and then the pre-thermalized stage with the transition to the thermalized equilibrium QGP. An important parameter of a strongly interacting QGP as a hot and dense liquid is the ratio η/s, where η is the viscosity and s is the entropy density. A small value of $\eta/s \geq 1/(4\pi)$ indicates the formation of the QGP state, which was actually observed in ALICE when describing transverse particle flows in the HKM model ($\eta/s = 0.08 \div 0.2$) [28].

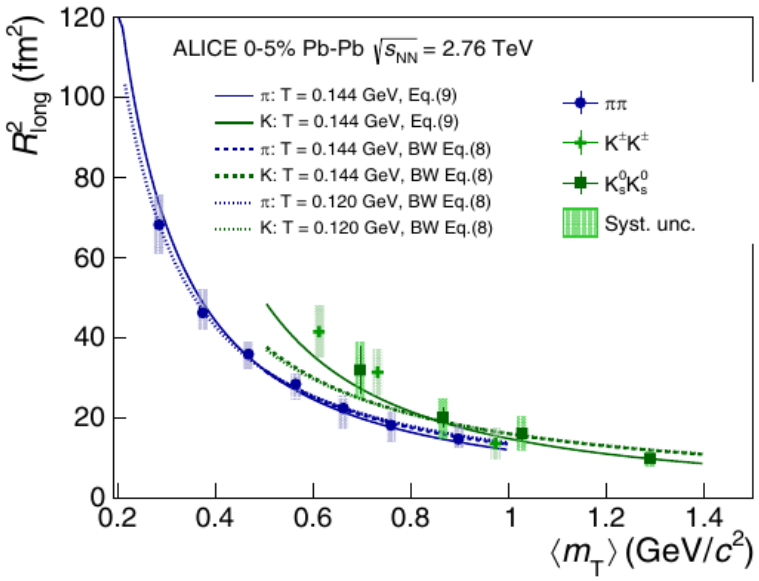

Fig. 8: The dependence of R^2_{long} on $\langle m_T \rangle$ for kaons and pions. The solid lines show the results of fitting with the Formula (3) used to determine the time of maximal particle emission τ_{max}. Dashed and dotted lines are explained in the text. T is the temperature value in the models.

A slightly higher R_{out}/R_{side} value for kaons than for pions indicates a longer duration of the kaon emission. To determine the time of maximal emission (τ_{max}), the formula proposed in [32] was used:

$$R^2_{long} = \tau^2_{max} \frac{T_{max}}{m_T \cosh y_T} \left(1 + \frac{3T_{max}}{2m_T \cosh y_T}\right), \quad (3)$$

where T_{max} is the temperature, all other parameters are explained in [5] in equation (9). The results of fitting the R^2_{long} dependences on $\langle m_T \rangle$ by Formula (3) are shown in Fig. 8 by solid lines for kaons and

pions and are in a good agreement with the experimental data. The obtained τ_{max} values are 12.40 ± 0.04 fm/s and 9.44 ± 0.02 fm/s for kaons and pions, respectively, which confirms a longer kaon emission. The dashed and dotted lines in Fig. 8 are the results of fitting with the formula (8) given in [5] and used in the earlier ALICE publication on the study of correlations of pion pairs [33]. It can be seen that such fit leads to results for kaons that are noticeably different from the experimental ones. The observed difference in τ_{max} for kaons and pions may be the cause of the m_T scaling violation discussed above. In [32], this difference is explained by the influence of $K^*(892)$ resonances with a lifetime of 4÷5 fm/s, formed during the rescattering of hadrons in the final state and decaying into charged kaons and pions. These kaons are up to 30% of all ones produced in nuclei collisions.

2.3. One-dimensional analysis of non-identical charged kaon femtoscopic correlations (K^+K^-) in Pb-Pb collisions at $\sqrt{s_{NN}}$ = 2,76 TeV [7].

As noted above, the sizes of particle emission sources can be determined through correlations of pairs of non-identical particles due to their interactions in the final state [13, 34]. Theoretical correlation function of K^+K^- pairs with relative momentum $\mathbf{k}^*$ in PRF and with total momentum (vector) $\mathbf{P}$ can be written as:

$$C_{sFSI}(\mathbf{k}^*,\mathbf{P}) = \int d^3\mathbf{r}^* S^{\alpha}(\mathbf{r}^*,\mathbf{P}) \sum_{\alpha'} \left|\psi^{\alpha'\alpha}_{-\mathbf{k}^*}(\mathbf{r}^*)\right|^2, \qquad (4)$$

where $\mathbf{r}^*$ is the relative distance between the points of emission of particles in the pair rest frame. The source function in a one-dimensional analysis is selected in a Gaussian form with a width R: $S(\mathbf{r}^*) \sim \exp(-\mathbf{r}^{*2}/4R^2)$. The index α denotes the K^+K^- channel, and the index α′ means the intermediate channels K^+K^-, $K^0\overline{K}^0$. The wave function of a pair of kaons is represented as a superposition of plane and spherical waves: $\psi_{-k^*}(r^*) = \exp(-ik^*r^*) + f(k^*)\exp(ik^*r^*)/r^*$. The scattering amplitude $f(k^*)$ of the K^+K^- pair is determined by the s wave of the isoscalar and isovector resonances $f_0(980)$ and $a_0(980)$, respectively, which are formed near the threshold, and can be written as a sum $f(k^*) = [f_0(k^*) + f_1(k^*)]/2$, where the first term refers to the f_0 resonance (isospin 0) and the second term refers to the a_0 resonance (isospin 1). The analytical functions $f_0(k^*)$ and $f_1(k^*)$ are presented in [7] by formulas (4) and (5), respectively, depending on the masses of resonances $f_0(980)$ and $a_0(980)$ and their coupling constants with various decay channels.

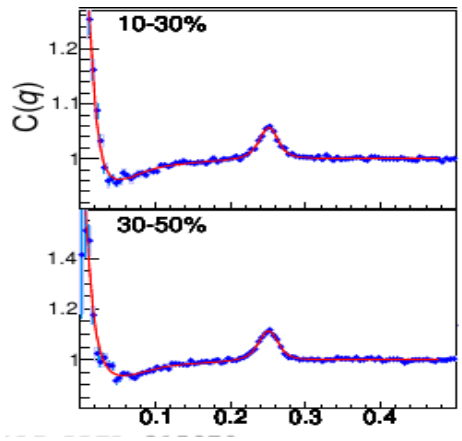

Fig. 9: Correlation functions of K^+K^- pairs for events of different centralities.

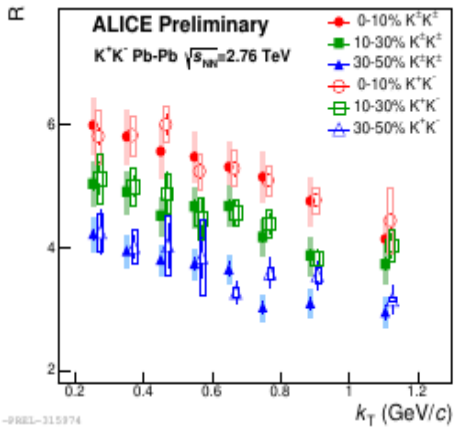

Fig. 10: Radii of kaon emission sources depending on k_T for events of different centralities.

When determining C_{sFSI}, the Coulomb interaction of charged particles [13] and the contribution of the

p wave of the strong interaction through the formation of the resonance ϕ(1020) [35] are also taken into account. Experimentally, the correlation functions were determined in the same way as indicated in Section 1 and are shown as an example in Fig. 9 for events of different centralities in the k_T (0.3 ÷ 0.4 GeV/c) interval. The main features of the correlation functions are as follows: the maximum from the Coulomb attraction at very small q < 0.05 GeV/c, the minimum at q ~ 0.05 GeV/c from the contributions of resonances $f_0(980)$ and $a_0(980)$, and ϕ(1020) meson peak around q = 0.25 GeV/c. The red line in Fig. 9 is the result of the fit using the numerically calculated theoretical correlation function discussed above. At the same time, the resonance parameters $a_0(980)$ were taken from the model [36] based on the analysis performed earlier in ALICE [37] (Achasov2 in Table 1 in [7]). The $f_0(980)$ resonance parameters were chosen (as free) under the condition that the values of the obtained femtoscopic radii were close to the values found in ALICE when analyzing pairs of identical charged kaons [2] according to the predictions of theoretical models. Figure 10 shows the femtoscopic radii obtained by the fit depending on k_T for events of different centralities. Here, for comparison, the radii found when studying pairs of identical kaons ($K^{\pm}K^{\pm}$ in the figure) are shown. As seen from the figure, the radii obtained in different analyses are in a good agreement with each other. As a result of fitting, the following values of the $f_0(980)$ resonance parameters were found [7]: mass m = 972 ± 3 ± 5 MeV/c^2, width Γ = 39.7 ± 7.94 ± 11.8 MeV, which correspond to the table Particle Data Group values.

3. One-dimensional analysis of femtoscopic correlations of identical charged kaon pairs in p-Pb collisions at $\sqrt{s_{NN}}$ = 5.02 TeV [6].

The study of femtoscopic correlations in p-A collisions is of interest primarily because this type of collision is intermediate between pp and A-A when studying the influence of hydrodynamic mechanisms on the size of the particle emission source. In one of the first theoretical works in the framework of the 3+1 hydrodynamic approach [38], a strong influence of these mechanisms was predicted in p-Pb collisions at LHC energies, leading to a noticeable increase in the size of particle emission sources compared to pp collisions. The same difference, although to a less extent, was predicted in the above-mentioned HKM model [39]. The study of pion correlations showed that in the one-dimensional analysis, the radii of the sources in the p-Pb and pp collisions coincide within uncertainties [40], and in the three-dimensional analysis they are also close, although with some difference for different three-dimensional projections [41]. Of unquestionable interest were similar studies of correlations of heavier particles, such as kaons, which were performed for the first time for p-A collisions by the JINR group.

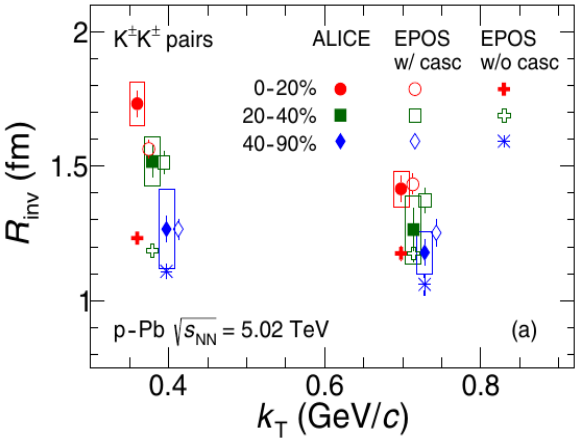

Fig. 11: Radii of kaon emission sources depending on k_T at different centralities. The results obtained in the EPOS model with (w/ casc) and without (w/o casc) the hadron rescattering cascade in the final state are compared.

For the analysis, all available data (~55 mln.) collected in p-Pb collisions at 5.02 TeV in 2013 were used. The experimental method and the analysis were the same as in the above sections and are

presented in more detail in [6]. Figure 11 shows R_{inv} of kaon emission sources depending on k_T for events of different centralities. The results obtained in the EPOS model with (w/ casc) and without (w/o casc) hadron rescattering cascade in the final state are presented. It can be seen, as in the case of Pb-Pb collisions (Fig. 7), that taking into account the rescattering of hadrons before the freeze-out leads to agreement of the model predictions with the experimental data. Figure 12 compares the dependences of the radii of the $K^{\pm}$ emission sources on the average multiplicity of charged particles $<N_{ch}>$ for various types of collisions. In the left figure, the results are taken from [6], where data obtained for Pb-Pb collisions at $\sqrt{s_{NN}}$ = 2.76 TeV were used for comparison. It can be seen from this figure that for the same values of $<N_{ch}>$, the radii in pp and p-Pb collisions coincide within uncertainties. These results are similar to those obtained for pions and mean that the statement of the above-mentioned models about a significantly stronger influence of the hydrodynamics mechanisms in p-Pb than in pp collisions is not confirmed.

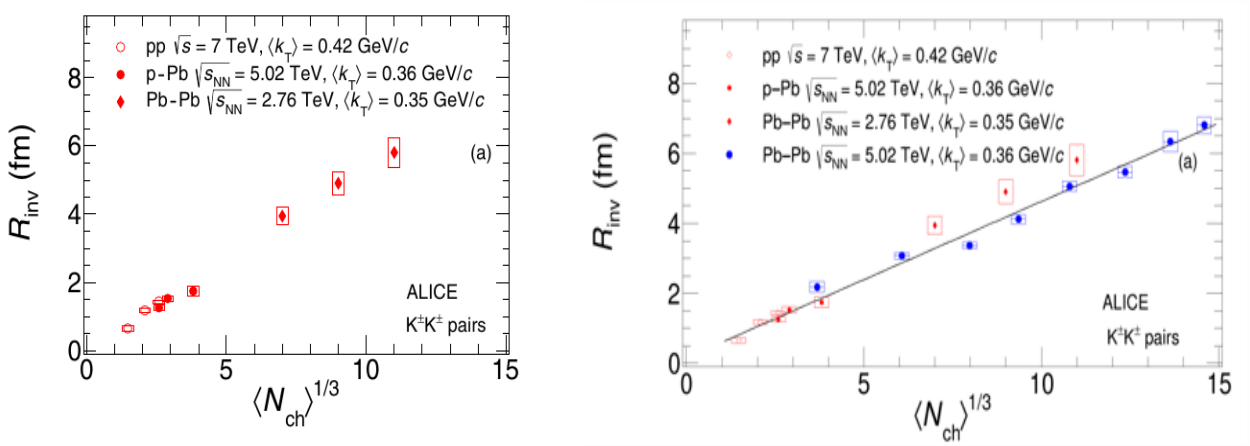

Fig. 12: Radii of $K^{\pm}$ emission sources depending on the average multiplicity of charged particles for different types of collisions. In the left figure, the results are taken from [6]. In the right figure, the results obtained for Pb-Pb collisions at $\sqrt{s_{NN}}$ = 5.02 TeV are added.

Figure 12 (left) also shows that a correct comparison with the results of Pb-Pb collisions cannot be made since small experimental data sets did not allow us to obtain radii at low N_{ch}, which is noted in the conclusions of [6]. Such comparison became possible for Pb-Pb collisions at $\sqrt{s_{NN}}$ = 5.02 TeV (Fig. 12, right) obtained later with much larger data set. Figure 12 (right) shows the preliminary values of the radii obtained in this case. These results were included in the master thesis of Romanenko G. E. (co-author of this presentation) and were reported by him at ALICE internal meetings. The figure shows that the new value of R_{inv} practically coincides, taking into account uncertainties, with the radius found for p-Pb collisions at the same N_{ch}, and the values for all types of collisions (except Pb-Pb at 2.76 TeV) fit well on one line, which is the result of fitting with a linear function. Some difference of the Pb-Pb results at 2.76 TeV from p-Pb ones does not seem significant enough taking into account the uncertainties. If these values are fit with the function f(x)= ax+b separately for Pb-Pb collisions and for pp and p-Pb ones, the parameters a = 0.47 ± 0.13, b = 0.67 ± 1.07 of the fit coincide within uncertainties with the parameters of the general pp, p-Pb and Pb-Pb fit which equal 0.42 ± 0.02 and 0.36 ± 0.18, respectively.

Conclusion.

In the presented cycle of works, femtoscopic correlations of charged kaon pairs formed in pp, p-Pb and Pb-Pb collisions at LHC energies were studied for the first time. It is worth emphasizing

that such studies have never been performed before in the proton-proton and proton-nucleus collisions even at lower energies. A number of new results were obtained, which can be summarized as follows:

– In proton-proton collisions, a significant difference was observed in the behavior of the radii of kaon emission sources at low and high multiplicities of charged particles. A similar result was obtained earlier in the study of charged pion femtoscopic correlations.

– The theoretically predicted m_T scaling for particles of various types was observed in Pb-Pb collisions for pairs of kaons and protons (antiprotons). However, it was not observed when comparing pairs of pions and kaons. This m_T scaling violation was explained in the framework of hydrokinetic models (HKM and EPOS) with the addition of a mechanism of the hadron rescattering in the final state.

– The kaon emission time measured in the HKM model exceeded the corresponding time found for pions, which was explained by the influence of different resonances who decay to these particles and was consistent with the observed violation of m_T scaling.

– The study of K^+K^- pairs in Pb-Pb collisions correlating due to final-state interactions allowed one to refine the f_0 resonance parameters by studying the strong interaction in the $K^+K^- \rightarrow f_0$ channel using the expected equality of the emission source sizes of identical and non-identical kaon pairs. The resulting mass and width of f_0 correspond to the PDG table values.

– The study of the identical charged kaon pair correlations in p-Pb collisions has shown that for the correct description of the source radii in the EPOS-3 model, similarly to Pb-Pb collisions, it is important to take into account the mechanism of hadron rescattering in the final state. In addition, comparing the obtained radii with those found in pp and Pb-Pb collisions, it can be concluded that the values of the radii are close in all three types of collisions at the same charged particle multiplicity. This result is different from the one obtained earlier in the $\pi^{\pm}$ study and requires further investigation within the framework of theoretical models.

– All the above results show that the properties of femtoscopic correlations of the considered particles formed in heavy-ion collisions are sufficiently well described by hydrodynamic models when considering several stages of nuclei interactions: the initial one – before the thermal equilibrium, the pre-thermalized stage with the transition to a thermalized equilibrium quark-gluon plasma, the hadronization stage taking into account the rescattering of particles in the final state. In pp and p-Pb collisions, the predictions of the models are not so unambiguous and need further understanding of how hydrodynamic mechanisms could influence particle production in these cases.

Bibliography.

9. E.V. Shuryak E.V. Phys. Rep. 61 (1980) 71-158.
10. S. Digal S. et al. Phys. Lett. B 549 (2002) 101-108.
11. S. Goldhaber et al. Phys.Rev 120 (1960) 300-3.
12. G. Kopylov, M. Podgoretsky. Sov. J. Nucl. Phys. 15 (1972) 219-223.
13. R. Lednicky, V. Lyuboshits. Sov. J. Nucl. Phys. 35 (1982) 770.
14. M.G. Bowler. Phys. Lett. B270, (1991) 69.; Y. Sinyukov et al. Phys.Lett. B432 (1998) 248.
15. K. Aamodt et al. (ALICE Collaboration), Phys. Rev. D84 (2011) 112004.
16. B. Abelev et al. (ALICE Collaboration), Phys. Lett B 717 (2012) 151.
17. S.Pratt. Phys. ReV. Lett. 53 (1984) 1219; M. Lisa et al. Annu. Rep. Nucl. Part. Sci. 55 (2005) 357.
18. K. Werner at al. Phys. Rev. C 83 (2011) 044915.

19. V. Khachatryan V. et al. (CMS Collaboration), JHEP 09 (2010) 091.
20. J. Adam et al. (ALICE Collaboration), Nature Phys. 13 (2017) 535-539.
21. T.J. Humanic. J. Phys. G 38 (2011) 124058.
22. S. Akkelin et al. Phys. Rev. C 65 (2002) 064904; B. Abelev et al. (ALICE Collaboration), Phys. Rev. C 89 (2014) 024911.
23. D.H. Rischke and M. Gyulessy. Nucl. Phys. A 608 (1996) 479.
24. D.H. Rischke. Nucl. Phys. A 610 (1996) 88c.
25. J. Adams et al. (STAR Collaboration), Phys. Rev. C71 (2005) 044906.
26. Iu.A. Karpenko, Yu.M. Sinyukov. Phys. Part. Nucl. Lett. 8 (2011) 9, 981.
27. J. Vredevoogd and S. Pratt. Nucl. Phys. A 830 (2009) 515C.
28. V. Yu. Naboka et al. Phys. Rev. C93 (2016) 024902.
29. M. A. Lisa et al. Annu. Rep. Nucl. Part. Sci. 55 (2005) 357.
30. A. Kisiel et al. Phys. Rev. C 90 (2014) 064914.
31. V.M. Shapoval et al. Nucl. Phys. A 929 (2014) 1.
32. Yu. M. Sinyukov et al. Nucl. Phys. A 946 (2016) 227.
33. K. Aamodt et al. (ALICE Collaboration), Phys. Lett. B696 (2011) 328.
34. R. Lednicky et al. Phys. Atom. Nucl. 61 (1998) 2050; S. Bekele and R. Lednicky. Braz. J. Phys. 37 (2007) 994.
35. R. Lednicky. Part. Nucl. Lett. 8 (2011) 965.
36. N. Achasov and A. Kiselev. Phys. Rev. D 68 (2003) 014006.
37. S. Acharya et al. (ALICE Collaboration), Phys. Lett. B774 (2017) 64; Phys. Lett. B790 (2019) 22.
38. P. Bozek and W. Broniowski. Phys. Lett. B 720 (2013) 250.
39. V. Shapoval et al. Phys. Lett. B 725 (2013) 139.
40. B. Abelev et al. (ALICE Collaboration), Phys. Lett B 739 (2014) 139.
41. J. Adam et al. (ALICE Collaboration), Phys. Rev. C 91 (2015) 034906.